frontiers | Frontiers in Agronomy

ORIGINAL RESEARCH
published: 14 June 2022
doi: 10.3389/fagro.2022.898870

Photoselective Shade Films Mitigate Heat Wave Damage by Reducing Anthocyanin and Flavonol Degradation in Grapevine (*Vitis vinifera* L.) Berries

Lauren E. Marigliano[1], Runze Yu[1†], Nazareth Torres[1†], Justin D. Tanner[1], Mark Battany[2] and Sahap Kaan Kurtural[1]*

[1] Department of Viticulture and Enology, University of California Davis, Davis, CA, United States, [2] University of California Cooperative Extension, San Luis Obispo, CA, United States

OPEN ACCESS

Edited by:
Francesco Spinelli,
University of Bologna, Italy

Reviewed by:
Antonio Cellini,
University of Bologna, Italy
Monica Boscaiu,
Universitat Politècnica de València, Spain

***Correspondence:**
Sahap Kaan Kurtural
skkurtural@ucdavis.edu

†Present addresses:
Runze Yu,
Department of Viticulture and Enology, California State University, Fresno, CA, United States
Nazareth Torres,
Departamento de Agronomía, Biotecnología y Alimentación, Universidad Pública de Navarra, Pamplona, Spain

Specialty section:
This article was submitted to Climate-Smart Agronomy, a section of the journal Frontiers in Agronomy

Received: 18 March 2022
Accepted: 09 May 2022
Published: 14 June 2022

Citation:
Marigliano LE, Yu R, Torres N, Tanner JD, Battany M and Kurtural SK (2022) Photoselective Shade Films Mitigate Heat Wave Damage by Reducing Anthocyanin and Flavonol Degradation in Grapevine (Vitis vinifera L.) Berries. Front. Agron. 4:898870. doi: 10.3389/fagro.2022.898870

Wine grape production is challenged by forecasted increases in air temperature and droughts due to climate change and photoselective overhead shade films are promising tools in hot viticulture areas to overcome climate change related factors. The aim of this study was to evaluate the vulnerability of 'Cabernet Sauvignon' grape berries to solar radiation overexposure, optimize shade film use for preserving berry composition. An experiment was conducted for two years with four shade films (D1, D3, D4, D5) with differing solar radiation spectra transmittance and compared to an uncovered control (C0). Integrals for leaf gas exchange and mid-day stem water potential were unaffected by the shade films in both years. At harvest, berry primary metabolites were not affected by treatments applied in either year. Despite precipitation exclusion during the dormant seasons in shaded treatments, and cluster zone temperatures reaching 58°C in C0, yield was not affected. Berry skin anthocyanin and flavonol composition and content were measured by C18 reversed-phase HPLC. In 2020, total skin anthocyanins (mg·berry^{-1}) in the shaded treatments were 27% greater than C0 during berry ripening and at harvest. Conversely, flavonol content in 2020 decreased in partially shaded grapevines compared to C0. Berry flavonoid content in 2021 increased until harvest while flavonol degradation was apparent from veraison to harvest in 2020 across partially shaded and control grapevines. Untreated control showed lower di- to tri-hydroxylated flavonol ratios closer to harvest. Our results provided evidence that overhead partial shading of vineyards mitigate anthocyanin degradation by reducing cluster zone temperatures and is a useful tool in combatting climate change in hot climate regions.

Keywords: climate change, heat wave, kaempferol, photosynthesis, plant water status, stomatal conductance, anthocyanin

INTRODUCTION

Grapevine (*Vitis. vinifera* L.) is a resilient and lucrative crop with a vast global distribution (Kurtural and Gambetta, 2021). Historically, climate and cultivar associations have developed regional wine identities that are commercially and culturally valued. However, steady increases in air temperature across the world's most famous growing regions have been observed since 1980, threatening to shift appropriate climatic growing conditions to regions located in higher latitudes and altitudes in search for cooler climates (Kurtural and Gambetta, 2021). Concern for shifting regional climates is based in the understanding that certain grape cultivars thrive in specific optimum air temperature regimes where wine quality is optimized. At the onset of global air temperature shift during the 1980s, wine quality ratings increased, presumably due to increased berry sugar concentration and riper flavors (Adelsheim et al., 2016; Kurtural and Gambetta, 2021). However, during the 2010s there was a marked plateau in wine quality ratings, indicating that there may be a tipping point at which wine quality will suffer as air temperatures continually increase (Kurtural and Gambetta, 2021). Consequently, for a region to adapt to ever-warming air temperatures without detrimental decreases in wine composition, mitigation strategies need to be developed.

Among grape berry secondary metabolites, flavonoids play important roles in berry and wine composition. Anthocyanins are responsible for berry and wine color (Savoi et al., 2017), while flavonols act as photoprotectants in plants, scavenging free oxygen radicals and preventing enzymatic reactive oxygen species, while also contributing to wine color through co-pigmentation with anthocyanins (Waterhouse et al., 2016). Flavonoids are produced through the phenylpropanoid pathway (Castellarin et al., 2007), which is responsive to environmental conditions, including solar radiation. It is understood that UV-B radiation induces flavonol biosynthesis (Martínez-Lüscher et al., 2014a) by activating *MYBF1*, the key transcription factor responsible for the regulation of flavonol biosynthesis enzymes including two *flavonol synthase (FLS)* genes, VvFLS4 and VvFLS5. This occurs *via* a signaling cascade derived from the photoreception of UV-B radiation by Ultraviolet Resistance Locus 8 (UVR8) homodimers (Matus, 2016). Likewise, selectively screening out excessive UV-A and UV-B with overhead shade films would result in appropriate molecular signaling for flavonoid biosynthesis (Matus, 2016). Previous work (Martínez-Lüscher et al., 2019; Torres et al., 2020; Torres et al., 2021; Torres et al., 2022) determined that flavonol profile in red skinned grape berry was a reliable biomarker for canopy architecture. In warm climates, net accumulation of flavonols might be impeded by flavonol temperature sensitivity (Martínez-Lüscher et al., 2019). Therefore, selectively removing NIR spectrum from berries would result in less flavonoid degradation due to reduced heat gain by the berry. If the grape berry was subjected to solar radiation overexposure and subsequent heat wave damage soon after sugar translocation into the berry, flavonol degradation occurred and kaempferol molar abundance in grape skins exceeded 8.6% (Martínez-Lüscher et al., 2019). Kaempferol molar abundance is the ratio of the molecule to the total flavonols in berry skin. Subsequently, kaempferol molar abundance exceeded this threshold between 540-570 $MJ{\cdot}m^{-2}$ of accumulated global radiation post-veraison (Martínez-Lüscher et al., 2019).

Grape berry composition is derived from a balance between primary and secondary metabolites (Castellarin et al., 2007). Ultimately, in hot climate viticulture regions, the clear sky days and concomitant berry temperature gains result in decoupling of sugar and flavonoid in grape berries (Spayd et al., 2002). Under optimal growing conditions, there is a direct relationship between sugar content and anthocyanin synthesis in grape, as some flavonoid synthesis genes such as LDOX and DFR, possess 'sucrose boxes' in their promoters, resulting in sugar-regulated gene expression (Vitrac et al., 2000; Gollop et al., 2001; Gollop et al., 2002). However, like flavonols, anthocyanins are also susceptible to chemical or enzymatic degradation at high temperatures while sugar accumulation is unaffected. Movahed et al. (2016) described a putative peroxidase gene VviPrx31 which may be responsible for anthocyanin degradation under high temperatures. The effect of sugar and anthocyanin decoupling on berry and wine composition was investigated where 'Cabernet Sauvignon' berries subject to leaf removal and shoot removal treatments were harvested at 24°Brix and vinified (Torres et al., 2020; Torres et al., 2021). Compared to untreated control, wines from leaf and shoot removal treatments had reduced color stability due to less anthocyanin hydroxylation as a function of higher temperatures and solar radiation exposure.

Efforts to reduce berry heat gain and through solar radiation exposure in vineyards with overhead and partial shading have been attempted but remain controversial in commercial wine grape vineyards. Cartechini and Palliotti (1995) demonstrated that average within-canopy temperatures in 'Sangiovese' grapevines decreased by approximately 2°C when covered with shade cloth transmitting 30% and 60% photosynthetically active radiation (PAR). Similarly, thin netting and plastic films covering 'Italia' grapevines reduced mid-day temperatures within the canopy at fruit height by about 6°C below air temperature. (Rana et al., 2004) Martínez-Lüscher et al. (2017) partially excluded solar radiation with colored polyethylene shade nets. They concluded that partial shading of the canopy produced quantifiable differences in berry microclimate by reducing canopy temperature by 4°C on the SW-facing side of the canopy. The authors attributed the highest anthocyanin content in the Black-40% shade net lessened anthocyanin degradation from lower canopy temperature. However, partial shading in these experiments failed to selectively omit harmful solar radiation from the fruit, but rather reduced total solar radiation exposure by 40% of the total radiation. The objective of this study was to selectively remove portions of solar radiation spectrum using overhead shade films in the vineyard, to mitigate the vulnerability of 'Cabernet Sauvignon' grape berry to solar radiation overexposure and optimize berry composition at harvest with desirable sugar accumulation and minimized flavonoid degradation.

MATERIALS AND METHODS

Meteorological Variables

Air temperature, and precipitation data were obtained from an onsite California Irrigation Management Information System

(CIMIS, station #77, Oakville, CA) weather station 160 m away from the experimental site. Seasonal air temperature accumulation was recorded as growing degree days (GDD). GDD were calculated as summation of GDD at each day from 1 April to 1 October as (daily maximum temperature - daily minimum temperature)/2 – 10, disregarding negative values (**Figure 1**). The number of days above 34°C and 40°C were counted for the 2020 and 2021 growing seasons (**Figure S1**).

Experimental Site and Plant Materials

The study was conducted at the University of California Davis, Oakville Experimental Vineyard using "Cabernet Sauvignon" (*Vitis vinifera* L.) clone FPS08 grafted onto 110 Richter rootstock. The grapevines were trained to bilateral cordons, vertically shoot positioned, and pruned to 30-single bud spurs. he grapevines were trained to bilateral cordons, vertically shoot positioned, and pruned to 30-single bud spurs. The grapevines were planted at 2.0 m × 2.4m (vine × row) and oriented NE to SW. Irrigation was applied uniformly from fruit set to harvest at 25% of crop evapotranspiration.

Experimental Design

The experiment was arranged in a randomized complete block with four replications. Four photoselective shade films (Daios S.a. Naousa, Greece) and an untreated control were installed in 3 adjacent rows on 12 September 2019. The shade films remained suspended over the vineyard until 20 October 2021. The shade films were 2 m wide and 11m long and were secured on trellising approximately 2.5 m above the vineyard floor. Each experimental unit consisted of 15 grapevines in 3 adjacent rows. Measurements were taken in the middle row, from three adjacent grapevines, leaving the distal plants as borders. The shade films had specific photoselective properties as indicated in (**Figure 2** and **Table 1**). The photoselective properties of the overhead shade films were measured with a spectroradiometer as previously reported (Martínez-Lüscher et al., 2017).

Cluster Microclimate

To characterize the maximum temperature gain of the clusters *in situ*, HOBO Pendant MX Temp/Light (MX2202) data loggers (Onset Computer Corp., Pocasset, MA, USA) were placed on the west side of the canopy and the data were collected every 15 minutes. After a sustained heat wave event, temperature data was downloaded from each treatment replicate and processed. The sensors were mounted on wooden stakes and placed at fruit zone height (96 cm above vineyard floor) at the middle vine of each experimental unit. Canopy temperature data was measured from fruit set 7 and 10 June 2020 and 2021 until harvest (9 September 2020, and 7 September 2021, respectively).

Canopy Architecture

Leaf area index (LAI) was measured using the smartphone-based application VitiCanopy coupled with an IOS system (Apple Inc., Cupertino, CA, USA) (De Bei et al., 2016). A 'selfie-stick' was used for ease to place the device approximately 75 cm below the canopy. The device was placed beneath the canopy perpendicular to the cordon. Leaf area was then derived to calculate the leaf area to fruit ratio.

Leaf Gas Exchange and Plant Water Status

Leaf net carbon assimilation (A_{net}), stomatal conductance (g_s) and intrinsic water use efficiency (WUE_i) were measured bi-weekly from anthesis to harvest using a portable infrared gas analyzer CIRAS-3 (PP Systems, Amesbury, MA, USA). The gas analyzer was set to a relative humidity of 40% and the reference CO_2 concentration was 400 µmol CO_2·mol^{-1}. One sun-exposed leaf from the main shoot axis of each experimental vine was

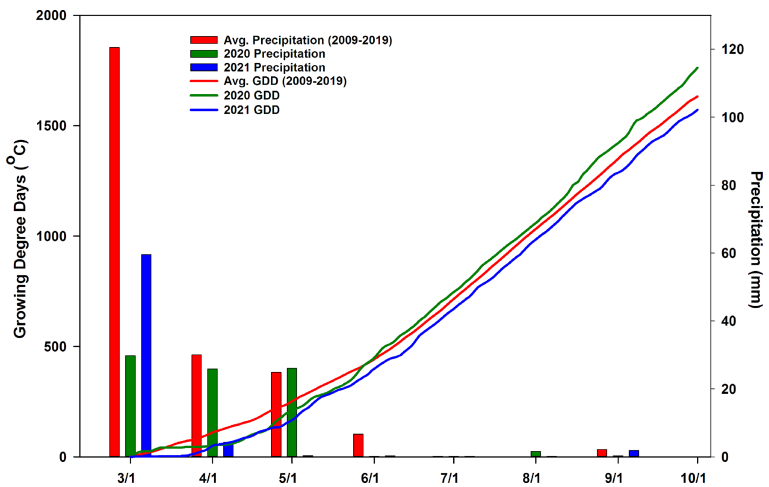

FIGURE 1 | Average precipitation and growing degree days (2009-2019) and experimental years (2020-2021) precipitation and growing degree days at Oakville, CA, USA during the water year (March-October).

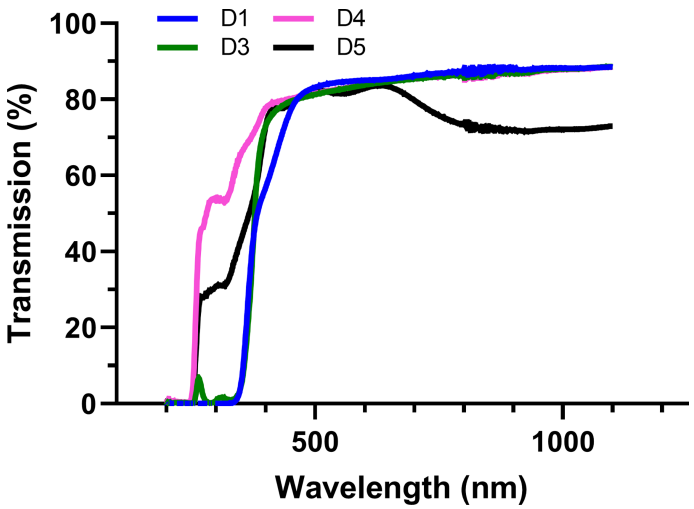

FIGURE 2 | Spectral transmittance (%) of shade films (D1, D3, D4, D5) and percentage of specific radiation spectra compared to open air.

selected and measured. Gas exchange measurements were taken at saturating light conditions.

Plant water status was measured as mid-day stem water potential (Ψ_{stem}) bi-weekly from anthesis until harvest each year. The Ψ_{stem} was measured at solar noon from 13:00 to 14:00 h. One leaf from the main shoot axis in the shade was selected and placed inside a pinch-sealed Mylar® bag 2 h prior to taking measurements. Measurements were taken using a pressure chamber (Model 615, PMS Instrument Company, Albany, OR, USA). The integrals for A_{net}, g_s, WUE_i and Ψ_{stem} were calculated by natural cubic splines for each parameter and calculating the area. The area divided by the number of days elapsed between the first measurement date and the last measurement date is the resulting integral values.

Yield Components

Grapes were harvested when they reached 25° Brix, as based on industry standards. Clusters from the three middle vines in each treatment replicate were removed by hand, counted, and weighed on a top-loading scale. The average cluster weight was calculated by dividing the crop weight by cluster number.

Fruit Sample Collection and Preparation

Seventy berries were collected each year at the following developmental stages: green berry, veraison, mid-ripening and at harvest and processed the same day. Berry weight was determined as the average of 70 berries. Fifty berries were separated for measuring berry primary chemistry parameters. The berries were crushed, and the resulting juice was used to measure total soluble solids (TSS) as degrees Brix using a digital refractometer (Atago PR-32, Bellevue, WA, USA). Titratable acidity (TA) and pH were measured using an autotitrator (862 Compact TitroSampler, Metrohm, Switzerland). Juice TA was expressed as g of tartaric acid per L of juice after titration to pH 8.3 with NaOH. Twenty berries were set aside and skinned by hand as previously reported (Martínez-Lüscher et al., 2019). Grape skins were collected and freeze-dried (Centrivap, Labcono, Kansas City, MO, USA). Once dried, the skins were ground into powder and 50 g of powder was extracted overnight at 4°C with methanol: water: 7M hydrochloric acid (70:29:1) for anthocyanin and flavonol quantification. Samples were centrifuged for 10 mins at 4000RPM. Supernatants were filtered (0.45µm; VWR, Seattle, WA, USA) and transferred to HPLC vials.

HPLC Procedures

Skin anthocyanins and flavonols were analyzed using a reversed-phase HPLC (Agilent model 1260, Agilent Technologies, Santa Clara, CA, USA) which consisted of a vacuum degasser, autosampler, quaternary pump and diode array detector with a column heater. A C18 reversed-phase column (LiChrosphere 100 RP-18, 4 x 520 mm^2, 5µm particle size, Agilent Technologies, Santa Clara, CA, USA) was utilized for flavonoid analysis as well. The mobile phase flow rate was 0.5 mL min^{-1}, and two mobile

TABLE 1 | Percent of solar radiation transmitted through the overhead shade films.

Treatment	Ultraviolet A	Ultraviolet B	Ultraviolet C	Photosynthetically active radiation	Near infrared
C0	100	100	100	100	100
D1	23.3	0	0	81.2	87.8
D3	25.9	1	1	81.9	87.1
D4	66.7	53.6	16.7	82.5	86.9
D5	48.2	30.8	9.7	81.2	73.2

phases were used, which included solvent A = 5.5% aqueous formic acid; solvent B = 5.5% formic acid in acetonitrile. The HPLC flow gradient started with 91.5% A with 8.5% B, 87% A with 13% B at 25 min, 82% A with 18% B at 35 min, 62% A with 38% B at 70 mins, 50% A with 50% B at 70.01 min, 30% A with 70% B at 75 min, 91.5% A with 8.5% B from 75.01 min to 91 min. The column temperature was maintained at 25°C. This elution allowed for avoiding co-elution of anthocyanins and flavonols as previously reported (Martínez-Lüscher et al., 2019). Flavonols and anthocyanins were detected by the diode array detector at 365 nm and 520 nm respectively. A computer workstation with Agilent OpenLAB (Chemstation edition, version A.02.10) was used for chromatographic analysis. Anthocyanins and flavonols were grouped into 3',4'-dihydroxylated and 3',4',5'-trihydroxylated species with regard to the B ring of the general flavonoid skeleton

Chemicals

All solvents were HPLC grade. Acetonitrile, methanol, hydrochloric acid and formic acid were purchased from Fisher Scientific (Santa Clara, CA, USA). Standards for flavonol identification (myricetin 3-*O*-glucoside, quercetin 3-*O*-glucuronide, quercetin 3-*O*-galactoside, quercetin 3-*O*-glucoside, kaempferol 3-*O*-glucoside, isorhamnetin 3-*O*-glucoside, and syringetin 3-*O*-glucoside) were purchased from Sigma-Aldrich (St. Louis, MO, USA). Oenin was purchased from Extrasynthese (Geney, France).

Statistical Analysis

Statistical analyses were conducted with R studio version 4.0.5 (RStudio: Integrated Development for R., Boston, MA, United States) for Windows. Seasonal integrals of Ψ_{stem} and gas exchange variables for each growing season and for both seasons were calculated by using the same software. All data were subjected to Shapiro–Wilk's normality test. Data were normally distributed and subsequently submitted to an analysis of variance (ANOVA) to assess the statistical differences between the overhead shade film treatments. For all data, means ± standard errors (SE) were calculated, and when the F value was significant ($p \leq 0.05$), Duncan's new multiple range *post hoc* test was executed using "agricolae" 1.2-8 R package (de Mendiburu, 2016).

RESULTS

Meteorological Conditions during Experimental Years

The weather conditions during the 2020 and 2021 growing seasons were compared to the long-term average for the study area over the past 10 years (2009-2019) (**Figure 1**). Compared to the past 10 years, the 2020 growing season accumulated more growing degree days by 1 October. Conversely, 2021 was a cooler growing season with less growing degree days accumulated than the long-term average. While GDD accumulation early in the season was similar during April – June for both years, the GDD accumulation in 2020 outpaced 2021, with 1762.7°C growing degree days accumulated in 2020 compared to 1572.3°C growing degree days accumulated in 2021. The total precipitation at the experimental site from 1 March 2020 to 30 September 2020 was 84.1mm. The 2020 water year experienced 100.5 mm less precipitation than the 10-year average for the experimental site. Particularly, the 2020 growing season experienced much less precipitation during March compared to the 10-year average with 1.2mm of precipitation accumulating in March 2020. Drought conditions continued into the 2021 water year, with 66.9 mm of precipitation between 1 March 2021 and 30 September 2021. Precipitation only occurred in March and April. Precipitation in the following months of 2021 was negligible. The number of days with maximum air temperature that exceeded 34°C and 40°C in 2020 and 2021 were different (**Figure S1**). In 2020, there were 32 days that exceeded 34°C while in 2021 there were only 22. Likewise, in 2020 there were 6 days that exceeded 40°C while in 2021 there was only one day that exceeded 40°C.

Primary Metabolism

The integrals for gas exchange and mid-day stem water potential were calculated (**Table 2**). In either year, there was no effect of overhead shade films on A_{net}, g_s or WUE_i or Ψ_{stem} integrals. Similarly, cluster number, yield per plant, and berry skin mass in both 2020 and 2021 were not affected by the shade films (**Table 3**). The LA : FR was not affected in either year of the trial.

Cluster Temperatures

Cluster temperatures were affected by overhead shade films during heat wave events. During heatwave events that occurred pre-veraison (11 July 2020), possible residual warming from the previous day resulted in warmer cluster temperatures in shaded treatments during the early morning hours (7:00h) (**Figure 3A**). Throughout the day, 2020 pre-veraison cluster temperatures in shaded and control treatments did not differ until 19:00h on 11 July, with the C0 having warmer clusters than all shaded treatments. Beginning at 9:00h on 11 July, cluster temperature in both shaded and control treatments was higher than ambient temperature for the remainder of the day. The largest warming effect (ΔT) on clusters occurred at 13:00h, with the temperature difference between C0 cluster temperature and ambient temperature being 13.3°C. The difference in D5 cluster temperature and ambient temperature was 9.8°C at solar noon. Cluster temperature trends were similar pre-veraison in 2021 (17 June 2021). However, differences in cluster temperature were only observed at 7:00h in 2021, again most likely residual warming effects from the previous day (**Figure 3C**). The largest ΔT was 11°C between D5 and ambient temperature at 15:00h.

The cooling effect of shade films on cluster temperature was more distinct during post-veraison heatwave events (**Figures 3B, D**). In the afternoon hours, cluster temperatures in shaded treatments were less than the control. In 2020, cluster temperatures under overhead shade films at 17:00h were at least 4°C cooler than clusters in C0 (**Figure 3B**). At 15:00h, ΔT between D3 and ambient temperature was 14°C, the largest

TABLE 2 | Effects of photo-selective overhead shade films on integrals of leaf gas exchange and mid-day stem water potential integrals on Cabernet Sauvignon/110R in Oakville, CA USA[ab].

Treatment	A_{net} (μmol CO_2 m^{-2}•s^{-1})	g_s (mmol H_2O m^{-2}•s^{-1})	WUE_i (μmol CO_2 •mmol H_2O^{-1})	Ψ_{stem} (MPa)
2020				
Control	10.56 ± 1.44	151 ± 22	0.073 ± 0.006	-1.10 ± 0.84
D1	8.78 ± 0.71	173 ± 24	0.058 ± 0.006	-1.03 ± 0.74
D3	9.56 ± 1.33	188 ± 29	0.055 ± 0.005	-1.04 ± 0.83
D4	9.28 ± 1.12	185± 36	0.058 ± 0.007	-1.11 ± 0.91
D5	9.47 ± 0.87	187 ± 36	0.061 ± 0.006	-1.05 ± 0.70
p value	n.s.	n.s.	n.s.	n.s.
2021				
Control	14.68 ± 1.37	182 ± 27	0.087 ± 0.010	-1.21 ± 0.11
D1	12.79± 0.84	187 ± 23	0.076 ± 0.009	-1.18 ± 0.11
D3	13.58 ± 1.00	196 ± 25	0.076 ± 0.010	-1.16 ± 0.10
D4	13.13 ± 1.01	185 ± 28	0.079 ± 0.010	-1.25 ± 0.11
D5	13.96 ± 0.91	202 ± 27	0.077 ± 0.010	-1.16 ± 0.09
p value	n.s.	n.s.	n.s.	n.s.

[a]*Values in each column are reported as mean ± standard error of the mean.*
[b]*n.s. indicates a p value ≥ 0.05.*

temperature difference observed on 18 August 2020. Similarly post-veraison C0 clusters in 2021 (28 August) consistently had higher cluster temperature compared to shaded clusters in the afternoon. Reduced cluster temperatures in shaded treatments compared to C0 were first observed midday (13:00h) and this cooling effect of the shade films continued throughout the afternoon until 17:00h (**Figure 3D**). During the warmest parts of the day (15:00h and 17:00h), the largest ΔT was 9°C between C0 and D4. C0 was 19.8°C warmer than ambient temperature at 15:00h, the hottest hour of the day. Regardless of transmission spectra, reduced solar spectra transmission significantly decreased cluster temperatures post-veraison.

Berry Weight and Juice Chemistry

In 2020, berry mass only differed between D3 and the control during post-veraison (**Figure 4A**). There was no significant difference in berry mass when measured pre-veraison. The differences among treatments for berry mass observed post-veraison were nonsignificant by mid-ripening and remained as such until harvest. TSS, pH and TA were also monitored throughout the growing season in both years. Overhead shade films did not affect TSS in must at any sampling point throughout the 2020 season (**Figure 4B**). TA was only significantly higher in D3 compared to the control, while pH was only significantly higher for the control when compared to D1. As berries developed, there was no significant effect of shade films on pH and TA (**Figures 4C, D**) compared to C0 from veraison until harvest.

Differences in berry mass occurred later in the season in 2021 compared to 2020 (**Figure 5A**). At mid-ripening, berry mass of D3, D4, D5 and C0 were similar and greater than that of D1. At harvest, shade films did not have any effect on berry mass. Unlike 2020, differences in TSS were observed at veraison and mid-ripening (**Figure 5B**). At veraison and mid-ripening, D3, D4, D5 and C0 had similar TSS. In 2021, D1 consistently differed from D5 at these sampling points for TSS. However, it had similar TSS as D4 and C0 at mid-ripening. There were no differences in TSS in between shade film and control fruit at harvest. Early season differences in pH were observed, with C0 having similar pH to D4 and D5

TABLE 3 | Effects of photo-selective overhead shade films on yield components of 'Cabernet Sauvignon/110R' in Oakville, CA, USA[ab].

Treatment	Yield (kg•$vine^{-1}$)	Skin weight (g)	Berry weight (g)	Leaf Area : Fruit (m^2•kg^{-1})
2020				
Control	5.10 ± 0.32	0.070 ± 0.01	0.894 ± 0.02	1.461 ± 0.222
D1	5.78 ± 0.52	0.054 ± 0.00	0.972 ± 0.05	1.612 ± 0.064
D3	5.60 ± 0.57	0.074 ± 0.01	0.919 ± 0.02	1.720 ± 0.084
D4	5.44 ± 0.41	0.065 ± 0.01	0.871 ± 0.01	1.840 ± 0.223
D5	5.34 ± 0.87	0.071 ± 0.00	0.901 ± 0.05	1.714 ± 0.306
p value	n.s	n.s.	n.s.	n.s.
2021				
Control	5.38 ± 0.67	0.067 ± 0.002	0.891 ± 0.07	0.941 ± 0.096
D1	5.86 ± 0.56	0.060 ± 0.008	0.962 ± 0.05	1.095 ± 0.072
D3	5.34 ± 0.28	0.065 ± 0.010	1.001 ± 0.01	1.587 ± 0.272
D4	5.53 ± 0.26	0.055 ± 0.007	0.925 ± 0.04	1.185 ± 0.190
D5	4.71± 0.53	0.069 ± 0.006	1.022 ± 0.10	1.499 ± 0.282
p value	n.s.	n.s.	n.s.	n.s.

[a]*Values in each column are reported as mean ± standard error of the mean.*
[b]*n.s. indicates a p value ≥ 0.05.*

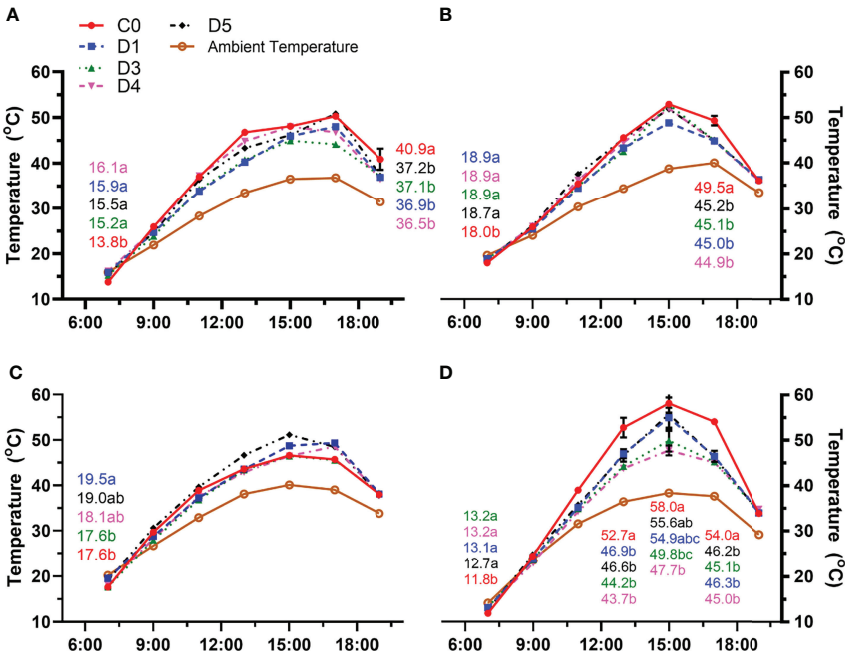

FIGURE 3 | Air temperature and cluster temperature of control (C0) and vines under shade films (D1, D3, D4, D5) recorded during heat wave events both pre-verasion and post-verasion. Temperatures were recorded pre-verasion on **(A)** 11 July 2020 and **(C)** 17 June 2021 and post-verasion on **(B)** 18 August 2020 and **(D)** 28 August 2021. Points are means ± standard error (n = 4).

(**Figure 5C**). When compared together, the shade films had similar pH at the green berry stage. There were no further differences in pH between treatments and control as ripening progressed. The TA only differed at mid-ripening with D1, D3 and C0 having the highest titratable acidities. D4 and D5 had similar TA, which was significantly less than D1 (**Figure 5D**). Titratable acidity did not differ between shaded and control fruit at harvest.

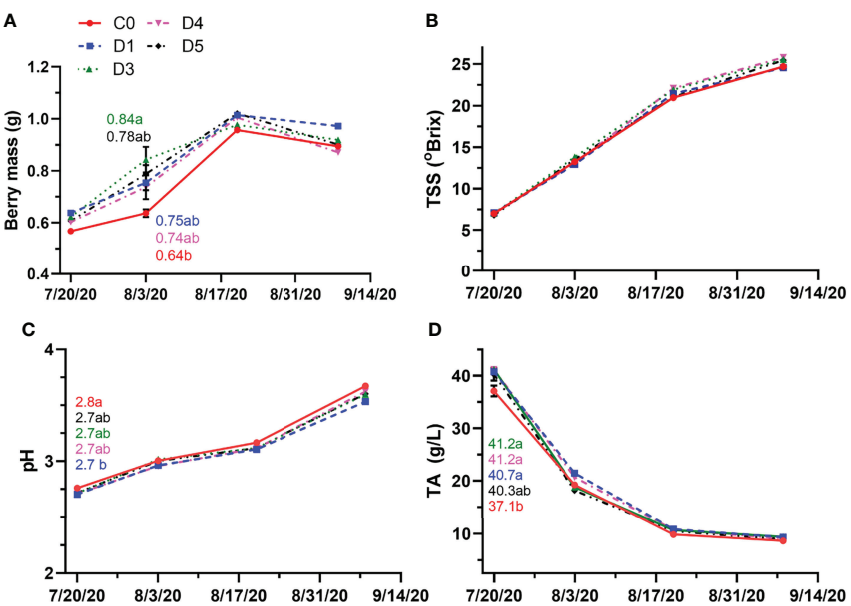

FIGURE 4 | Berry mass **(A)**, TSS **(B)**, pH **(C)** and TA **(D)** throughout berry development in 2020 for untreated (C0) and shade film treatments (D1, D3, D4, D5). Points are means ± standard error (n = 4). Means with no letters in common are significantly different ($p \leq 0.05$).

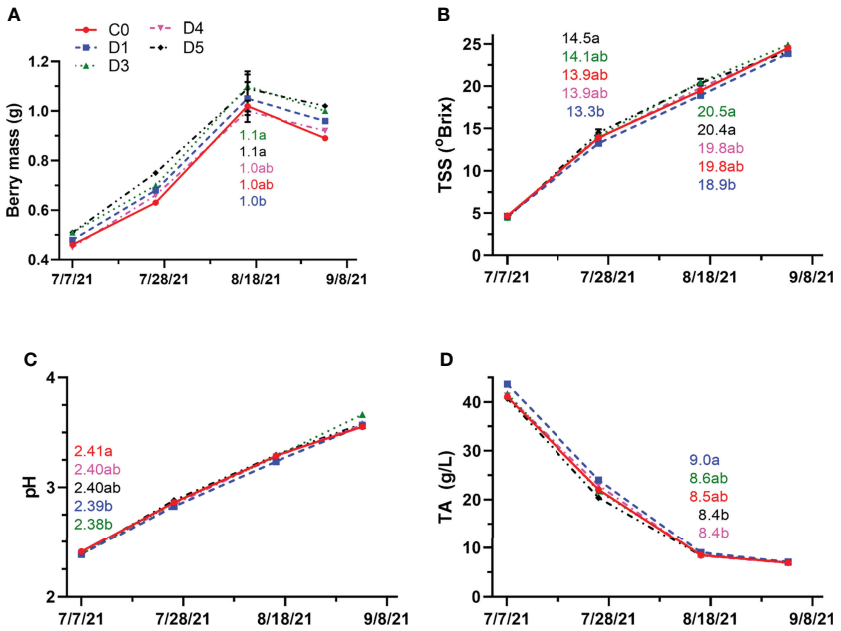

FIGURE 5 | Berry mass **(A)**, TSS **(B)**, pH **(C)** and TA **(D)** throughout berry development in 2021 for untreated (C0) and shade film treatments (D1, D3, D4, D5). Points are means ± standard error (n = 4). Means with no letters in common are significantly different ($p \leq 0.05$).

Skin Flavonoid Content

Compared to the control, grape berries grown under shade film had higher skin anthocyanins at both mid-ripening and harvest (**Figure 6A**) in 2020. In all treatments, total skin anthocyanin content peaked at mid-ripening and then decreased from mid-ripening to harvest, with D5 showing the smallest decrease in total skin anthocyanin content (**Figure 6A**). However, the shade treatment films resulted in 27% greater anthocyanin content than C0 at harvest. The proportion of tri-hydroxylated anthocyanins increased throughout berry development in all treatments (**Figure 6C**). However, shade films did not affect anthocyanin proportion of hydroxylation compared to the control in this year (**Figure 6C**).

In 2020, total skin flavonol content increased in both shaded treatments (D1, D3, D4, D5) and the unshaded control (C0) until the veraison (**Figure 6B**). However, C0 consistently had higher flavonol content compared to shaded treatments. Between the shaded treatments, D4 and D5 produced fruits with significantly more flavonol content per berry compared to D1 and D3 at each sampling time point, except at immediate pre-veraison, where flavonol content in D4 was not significantly different compared to D1 and D3. At mid-ripening flavonol content decreased in both shaded and unshaded fruits. At harvest, there was no significant difference in flavonol content between C0, D4, and D5. Shade films D1 and D3 had less total skin flavonols than C0, D4 and D5, containing approximately 0.06 mg/berry. The proportion of tri– to di-hydroxylated flavonols was affected by the overhead shade films (**Figure 6D**). At mid-veraison, there was a greater proportion of tri-hydroxylated flavonols with D1 and D3 compared to D4, D5, and C0. The differences between treatments were pronounced at harvest in 2020 with C0 resulting with the least amount of tri-hydroxylated flavonols in 2020.

In 2021, differences in total skin anthocyanin content were evident at veraison and mid-ripening (**Figure 7A**). At veraison, total skin anthocyanin content was higher in D5 compared to D1. Shade films C0, D3, and D4 had similar total skin anthocyanin content to D1 and D5 at veraison. At mid-ripening, D5 has significantly higher total skin anthocyanin content to C0, with D1, D3 and D4 having similar anthocyanin content. At harvest, overhead shade films did not have an impact on total skin anthocyanin content. However, anthocyanin content increased from mid-ripening to harvest in D1, D3 and D4, while they appeared to reach a plateau in anthocyanin content in D5 and C0. The effects of overhead shade films on anthocyanin hydroxylation were only observed at mid-ripening with D1 having higher proportions of 3',4',5' to 3',4'- hydroxylated anthocyanins than D4 and D5, and C0 along with D3 did not differentiate with other treatments (**Figure 7C**).

In 2021, the accumulation trend of skin flavonol content differed compared to that of 2020. At the first sampling point, total skin flavonols were the highest in C0 while D1 had the lowest flavonol content (**Figure 7B**). The flavonol content continued to increase as ripening progressed. From mid-ripening to harvest, C0, D5 and D4 had the highest flavonol content compared to D1 and D3. In 2021, total skin flavonols did not decrease prior to harvest. The seasonal trend of di- to tri-hydroxylated flavonols differed in 2021 compared to 2020. Early in the season, D1 and D3 had more tri-hydroxylated flavonols (**Figure 7D**). From veraison to harvest D1, D3 and D5 had more tri-hydroxylated flavonols compared C0. Similar to 2020, C0 consistently had the lowest ratio of tri- to di-hydroxylated flavonols at every sampling point with the difference at harvest.

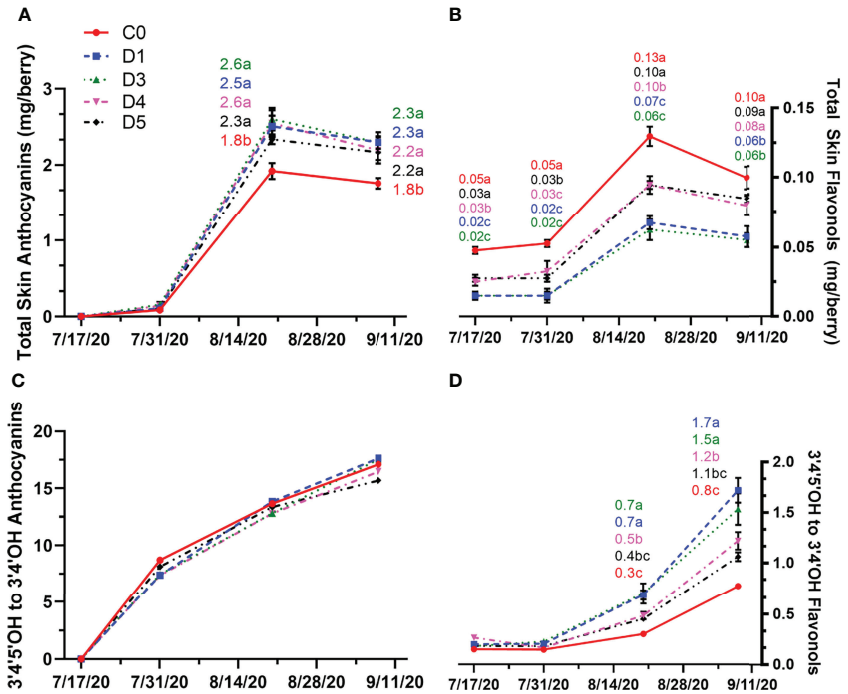

FIGURE 6 | Total skin anthocyanin **(A)** and flavonol **(B)** content and anthocyanin **(C)** and flavonol **(D)** hydroxylation profile (ratio of 3'4'-OH and 3'4'5'-OH) throughout berry development in untreated (C0) and shade film treatments (D1, D3, D4, D5) in 2020. Points are means ± standard error (n = 4). Means with no letters in common are significantly different ($p \leq 0.05$).

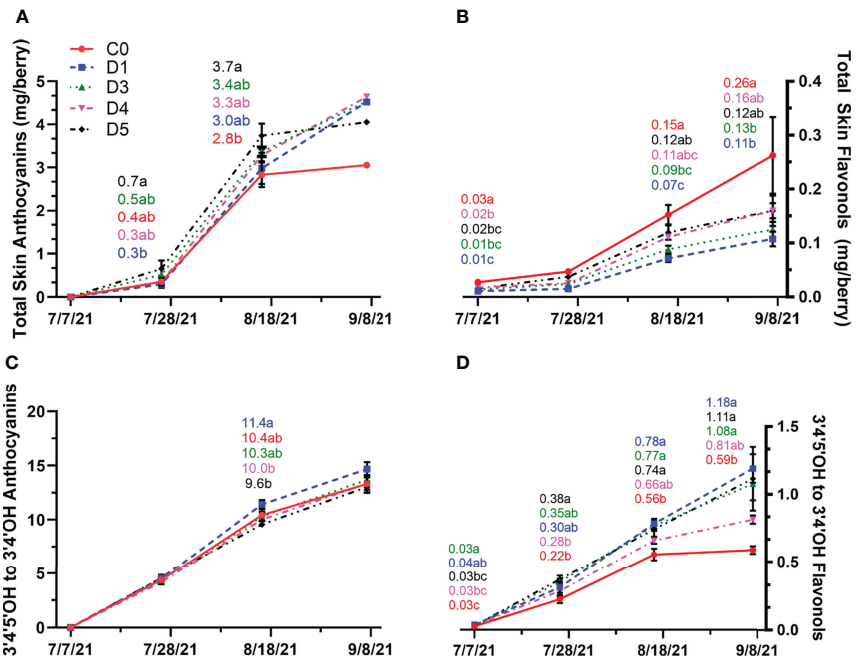

FIGURE 7 | Total skin anthocyanin **(A)** and flavonol **(B)** content and anthocyanin **(C)** and flavonol **(D)** hydroxylation profile (ratio of 3'4'-OH and 3'4'5'-OH) throughout berry development in untreated (C0) and shade film treatments (D1, D3, D4, D5) in 2021. Points are means ± standard error (n = 4). Means with no letters in common are significantly different ($p \leq 0.05$).

In 2020, molar abundance of kaempferol peaked at mid-ripening (**Figure 8A**). C0 had the highest molar abundance of kaempferol. The molar abundance of kaempferol in D5 was significantly higher compared to D1 and D3. A decrease in kaempferol molar abundance was observed from mid-ripening to harvest. Nevertheless, at harvest, molar abundance of kaempferol remained the greatest in C0 compared to the other overhead shade films, and D1 had the lowest kaempferol molar abundance. In 2021, the molar abundance of kaempferol increased until mid-ripening and then appeared to either level off or decrease from mid-ripening to harvest in all treatments (**Figure 8B**). Differences in molar abundance of kaempferol were observed at veraison and mid-ripening but not at harvest. At veraison and mid-ripening, C0 had more kaempferol than D1 and D3. Similar molar abundance of kaempferol was observed betweenD5 and other treatments at verasion, and D4 and other treatments at mid-ripening.

DISCUSSION

Precipitation, Heat Waves and Overhead Shade Films

The weather in 2020 and 2021 varied considerably leading to year-to-year variation in the study. In 2020, the air temperatures were higher than the long-term 20-year average for Oakville, CA. In previous studies at this experimental site, similar heat wave events were recorded. In 2017 there were 7 days above 40°C and 64 days above 30°C (Martínez-Lüscher et al., 2017). Conversely, 2021 was a cooler growing season than the 20-year average and recent past years. Compared to precipitation trends of the past 20 years, 2020 and 2021 were severe drought years. The yearly variation in temperatures and precipitation in this study helps to exemplify the unpredictability of growing conditions forecasted with climate change. The application of solar radiation exclusion may become increasingly necessary for wine grape production in hot climates to maintain optimal berry and wine chemistry.

Reduction of Berry Temperature

Ponce de León and Bailey (2021) quantified berry temperature in a VSP trellis system using thermocouples and subsequently modelled berry temperature temporally and spatially. In an uncovered VSP trellis system, black grape berries in direct sunlight can reach temperatures over 10°C above ambient temperatures with the hottest hours being from 15:00h to 17:00h, while naturally shaded fruits followed ambient temperature (Ponce de León and Bailey, 2021). Similarly, Martínez-Lüscher et al. (2017) found that sun exposed grape berries reached temperatures approximately 15°C warmer than ambient air in the afternoon. We observed a temporal shift in the efficacy of overhead shade films. Prior to veraison, overhead shade films did not reduce cluster temperatures, as green berries do not absorb as much heat as black berries after verasion. However, shaded berries were still warmer than ambient temperature which conflicted with the assumptions from the model presented by Ponce de León and Bailey (2021). After veraison, the cooling effect of shading film was evident as black berries absorbed heat. Shade films in 2020 exceeded the performance of black shade netting with 40% shade factor used by Martínez-Lüscher et al. (2017). Partial shading with black shade netting reduced cluster temperature of cluster temperature by 3.7°C, while overhead shade films reduced cluster temperature by at least 4°C compared to uncovered control vines. During a heatwave post-veraison in 2021, berry temperatures reached a maximum temperature of 58°C in C0, which was the highest recorded berry temperature in both years. At this temperature extreme, shade films were effective in reducing berry temperature. Even when the berry temperatures did not reach this extreme temperature, overhead shade films performed with a similar cooling effect. The cooling effect on clusters results from the shielding of grapes from NIR, which minimized the heat load on the clusters in the afternoon hours. While D4 was the most effective at reducing cluster temperature when maximum temperatures were reached, D5 optimized flavonoid development by balancing heat reduction and solar radiation exclusion. This balance was achieved with the reduction of NIR transmission by approximately 27%.

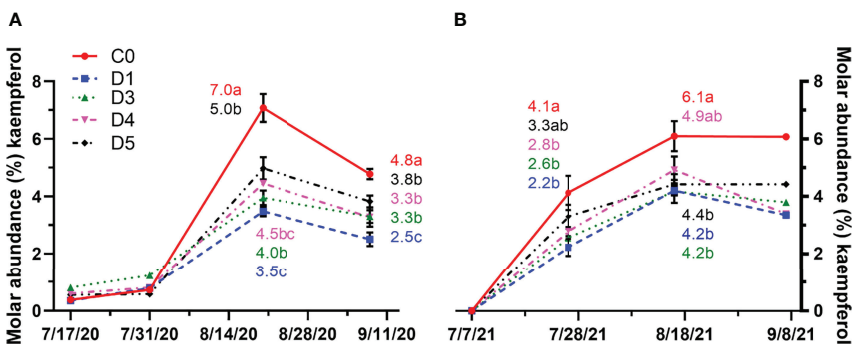

FIGURE 8 | Molar abundance (%) of kaempferol throughout the growing season in **(A)** 2020 and **(B)** 2021 for untreated vines (C0) and vines under shade film treatments (D1, D3, D4. D5). Points are means ± standard error (n = 4). Means with no letters in common are significantly different ($p \leq 0.05$).

Gas Exchange, Leaf Area and Plant Water Status

Grapevine physiological responses to reduced photosynthetically active radiation (PAR) *via* shading in hot climates have been reported. Previous work with partial shading *via* colored shade nets reduced total solar radiation by 40%, without selecting specifically for PAR reduction and found no differences in net carbon assimilation, stomatal conductance, leaf water potential and most importantly, yield (Martínez-Lüscher et al., 2017). When calculated as season-long integrals, overhead shade films had no effect on photosynthetic parameters. This may be attributed to the transmission spectra of the polyethylene shade films. Each shade film reduced PAR transmission by approximately 20% from full transmission. The photosynthetic capacity of grapevines is optimized between 800 and 1200 $\mu mol \bullet m^{-2} s^{-1}$ of solar radiation (Carvalho et al., 2016), despite 2000 $\mu mol \bullet m^{-2} s^{-1}$ of solar radiation provided under control conditions. Since leaf area was maintained across treatments and PAR was only reduced by 20%, the photosynthetic capacity of the grapevines was unaltered under the shade films. Negligible differences in canopy size and the replacement of 25% ET_c resulted in no significant effect on Ψ_{stem} or g_s integrals between treatments within a given year. However, C0 and D4 in both years were trending towards more negative Ψ_{stem} values, which may be due to larger transmittance of NIR radiation and increased evaporative demand. Similar effects on plant water status and gas exchanges were observed by shading *via* shade nets when canopy size was maintained across treatments (Martínez-Lüscher et al., 2017). By maintaining aspects such as canopy size and plant water status required for adequate ripening across the treatments (Bergqvist et al., 2001), the effects of shading on berry composition were most likely related to the fruit zone microclimate, specifically reduction of temperature.

Berry Size and Composition

Plant organ development relies on a balance of carbon and water availability (Keller, 2020). At low doses, ultraviolet light reduces cell division and expansion (Robson et al., 2015). However, previous studies indicated that berry size is unaffected by changes in solar radiation, alterations in amounts of specific wave bands, or temperature (Spayd et al., 2002; González et al., 2015). Rather, berry size is a function of cluster compactivity (number of berries per cluster) and the amount of irrigation (Keller et al., 2016). As our applied water amounts and cluster count were constant in both shaded and control treatments, berry size was unaffected. Consequently, yield was unaffected by overhead shade films as well.

Grapevine phenology and berry ripening are thermally regulated (Keller, 2020). In our experiment, temperature and solar radiation were coupled. However, changes to temperature caused by the overhead shade films were not enough to result in changes in berry TSS accumulation in both years. Regardless of shading, grape berries reached the commercial winemaking standard of 25 °Brix. While this desired sugar concentration is often attained in hot vineyard climates, the decoupling of sugar and anthocyanin development driven by heat waves may cause issues with achieving commercial wine expectations, leading to higher alcoholic wines with immature flavonoid composition (Martínez-Lüscher et al., 2014a; Torres et al., 2022).

Tartaric and malic acids are present in the grape berry at all developmental stages (Keller, 2020). As the berry ripens, malic acid accumulates until a metabolic shift at veraison. After verasion, the berry loses malic acid to cellular processes such as respiration and gluconeogenesis (Sweetman et al., 2014). Elevated temperature has been shown to reduce must acidity (Spayd et al., 2002). Ultimately the loss of malic acid from increased temperature is demonstrated to be due to increased degradation rather than reduced pre-veraison biosynthesis (Sweetman et al., 2014). Must acidity values as low as 4.66 $g \bullet L^{-1}$ have been reported in a hot climate region as the San Joaquin Valley, California in Merlot grapes under pre-bloom mechanical leaf removal (Cook et al., 2015). In this study, must acidity and pH at harvest were not affected by overhead shade films. Rather, titratable acidity and pH at harvest in 2020 were maintained at previously reported levels from the experimental site, despite a warmer than average growing season, where approximately 500 more GDDs accumulated in 2020 than those previously reported by Martínez-Lüscher et al. (2017). Despite higher recorded GDD in the present study, titratable acidity at harvest was maintained around 7 $g \bullet L^{-1}$. Ultimately the reduction in cluster temperature imparted by the shading impeded organic acid degradation therefore maintaining berry acidity.

Effects on Flavonoids

Anthocyanins are the products of the phenylpropanoid pathway. The phenylpropanoid pathway is controlled by a suite of structural genes including *chalcone synthase* (*CHS*) and *flavonoid-3-O-glucotransferase* (*UFGT*) at the beginning and end of the pathway, respectively (He et al., 2010). Anthocyanin biosynthesis is triggered by a sugar stimulus, resulting in a modification of *UFGT* expression (Wu Dai et al., 2014). Previous work has identified a multitude of MYB-related transcription factors including VvMYBA1, VvMYBA2, VIMYBA1-2, VIMYBA1-3 AND VIMYBA2 as being temperature and light responsive in upregulating anthocyanin biosynthesis (Kobayashi et al., 2002; Kobayashi et al., 2004; Walker et al., 2007; Azuma et al., 2008). However, there was evidence to support anthocyanin downregulation with high temperatures *via* repression of *UFGT* by MYB4 (Mori et al., 2007). Anthocyanin compounds are also temperature sensitive and will degrade when temperatures exceed 35°C (Mori et al., 2007). Optimum temperature thresholds were established for anthocyanin accumulation in grape berries. It was identified that anthocyanin accumulation was maximized at 875 GDD and a daily mean light intensity of $220 klm \cdot m^{-2}$ after which anthocyanin content decreased in Cabernet Sauvignon (Torres et al., 2020). Previous works that used partial shading that transmitted 60% of solar radiation had also resulted in increased anthocyanin content compared to unshaded fruit in under similar growing season and climatic conditions (Reshef et al., 2017). In 2021, shade films did not affect the anthocyanin content in berry skins at harvest, due to the cooler growing season limiting anthocyanin degradation post-veraison. The reduction in anthocyanin content observed in 2020 may result from repressed anthocyanin biosynthesis at hot temperatures *via* the MYB4 repressor (Mori et al., 2007).

However, it is also highly likely that elevated temperatures in 2020 resulted in increased anthocyanin degradation in exposed fruit compared to shaded fruit, leading to shaded fruit having greater anthocyanin content.

Flavonols are photoprotectants and free radical scavengers in the plant kingdom (Martínez-Lüscher et al., 2014b). As such, these compounds are directly responsive to light exposure of the cluster. In the phenylpropanoid pathway, MYBF1 is a transcriptional regulator of FLS, the key gene in flavonoid synthesis (Czemmel et al., 2009). It has been shown that MYBF1 is upregulated by UV-B light, resulting in increased flavonols in grape berry skins (Martínez-Lüscher et al., 2014b). Thresholds for optimal sunlight exposure have been elucidated in previous solar radiation exclusion experiments, where Martínez-Lüscher et al. (2019) tracked flavonol development over the growing season under 20% and 40% shading conditions. It was determined that net flavonol biosynthesis occurs until approximately 570 MJ m^{-2} of accumulated global radiation which corresponds with 7.6% molar abundance of kaempferol in grape skins (Martínez-Lüscher et al., 2019). Beyond these thresholds, flavonols started to be degraded in the grape berries. Our study showed a similar trend for flavonol content in hot years like 2020. The control treatments in 2020 exceeded 8.6% kaempferol abundance, while shade films were effective in maintaining kaempferol abundance below this overexposure threshold. In cooler years like 2021, flavonol degradation was not observed at the global radiation threshold as a result of the cooler growing season. Rather, biosynthesis continued to increase flavonol content until harvest in 2021. Shade films effectively lengthened the period of flavonol biosynthesis and reduced the amount of time during ripening where clusters are under flavonol degrading conditions.

Anthocyanins are comprised of two aromatic rings (the A-ring and B-ring) linked by three carbons in an oxygenated heterocycle (Bueno et al., 2012). Hydroxylation and methylation of the B- ring is responsible for color and hue of each anthocyanin molecule. Increasing free hydroxyl groups on the B-ring enhances blueness while methylation of the hydroxyl groups increases redder hues in grape skins (He et al., 2010). From a winemaking perspective, 3'4'5-OH anthocyanins are more resistant to degradation during fermentation, leading to stable wine color (Gómez-Plaza et al., 2008). In this study, overhead shade films did not affect anthocyanin hydroxylation by harvest in either year of this study. However, shifts in anthocyanin hydroxylation have been previously documented: colored shade nets (blue and black) reducing solar radiation by 40%, showed higher anthocyanin and flavonol hydroxylation compared to unshaded treatments (Martínez-Lüscher et al., 2017). Previous studies reported increases in the ratio of di-tri hydroxylated anthocyanins in grapevines under water deficits (Castellarin et al., 2007; Cook et al., 2015; Savoi et al., 2017). The absence of this shift in anthocyanin hydroxylation under shade films was most likely due to similar grapevine water status among the shaded and control treatments, as the vines were not under water deficit conditions. However, shade films altered flavonol hydroxylation under hot growing conditions in 2020, with hydroxylation being the highest in the least exposed shade films (D1 and D3). Shade films D4 and D5 transmitted 60% and 40% of UV-B radiation respectively, resulting in less flavonol hydroxylation than D1 and D3, but more hydroxylation than the control. In cooler growing conditions in 2021, all shade films had comparable levels of flavonol hydroxylation, yet hydroxylation was still greater under shade films than the control. These results may be due to the upregulation of flavonoid 3' hydroxylase (F3'H). This enzyme is responsive under sun exposure and is responsible for the generation of 3'4' hydroxylated flavonoid precursors. (Martínez-Lüscher et al., 2014a).

CONCLUSIONS

In the context of climate change, more frequent heat wave events may be deleterious on grape and wine quality. This study aimed to elucidate the optimal solar spectrum to avoid deleterious impacts on grapevine physiology and berry composition associated with increased temperatures. Overhead shade film D5 effectively reduced cluster temperature by blocking near infrared radiation resulting in 27% greater anthocyanin content. Grapevine water status, leaf gas exchange and berry primary chemistry were maintained underneath overhead shade films. Anthocyanin content was increased under shade films in warmer than average years, ultimately due to reduced degradation from excessive cluster temperatures. Shade film D5 produced temperature and solar radiation conditions which optimized berry flavonoid content. Overhead shade films are a novel solution for grape producers in hot climate viticultural regions, as more frequent heat wave events are forecasted with climate change.

DATA AVAILABILITY STATEMENT

The raw data supporting the conclusions of this article will be made available by the authors without undue reservation.

AUTHOR CONTRIBUTIONS

SK designed the study and acquired the funding. LEM, RY, NT, JT executed the trial. LEM, RY, NT and JT collected, and curated the data. LEM wrote the first draft of the manuscript. All authors contributed to the writing of the manuscript and approved the final version.

FUNDING

A graduate student stipend was provided to LM from University of California Davis during the execution of the trial.

SUPPLEMENTARY MATERIAL

The Supplementary Material for this article can be found online at: https://www.frontiersin.org/articles/10.3389/fagro.2022.898870/full#supplementary-material

REFERENCES

Adelsheim, D., Busch, C., Catena, L., Champy, B., Coetzee, J., Coia, L., et al. (2016). Climate Change: Field Reports From Leading Winemakers. *J. Wine Econ.* 11, 5–47. doi: 10.1017/jwe.2016.4

Azuma, A., Kobayashi, S., Mitani, N., Shiraishi, M., Yamada, M., Ueno, T., et al. (2008). Genomic and Genetic Analysis of Myb-Related Genes That Regulate Anthocyanin Biosynthesis in Grape Berry Skin. *Theor. Appl. Genet.* 117, 1009–1019. doi: 10.1007/s00122-008-0840-1

Bergqvist, J., Dokoozlian, N., and Ebisuda, N. (2001). Sunlight Exposure and Temperature Effects on Berry Growth and Composition of Cabernet Sauvignon and Grenache in the Central San Joaquin Valley of California. *Am. J. Enol. Vitic.* 52, 1–7. doi: 10.3923/rjss.2014.31.38

Bueno, J. M., Sáez-Plaza, P., Ramos-Escudero, F., Jiménez, A. M., Fett, R., and Asuero, A. G. (2012). Analysis and Antioxidant Capacity of Anthocyanin Pigments. Part II: Chemical Structure, Color, and Intake of Anthocyanins. *Crit. Rev. Anal. Chem.* 42, 126–151. doi: 10.1080/10408347.2011.632314

Cartechini, A., and Palliotti, A. (1995). Effect of Shading on Vine Morphology and Productivity and Leaf Gas Exchange Characteristics in Grapevines in the Field. *Am. J. Enol. Vitic.* 46, 227–234.

Carvalho, L. C., Coito, J. L., Gonçalves, E. F., Chaves, M. M., and Amâncio, S. (2016). Differential Physiological Response of the Grapevine Varieties Touriga Nacional and Trincadeira to Combined Heat, Drought and Light Stresses. *Plant Biol.* 18, 101–111. doi: 10.1111/plb.12410

Castellarin, S. D., Matthews, M. A., Di Gaspero, G., and Gambetta, G. A. (2007). Water Deficits Accelerate Ripening and Induce Changes in Gene Expression Regulating Flavonoid Biosynthesis in Grape Berries. *Planta* 227, 101–112. doi: 10.1007/s00425-007-0598-8

Cook, M. G., Zhang, Y., Nelson, C. J., Gambetta, G., Kennedy, J. A., and Kurtural, S. K. (2015). Anthocyanin Composition of Merlot is Ameliorated by Light Microclimate and Irrigation in Central California. *Am. J. Enol. Vitic.* 66, 266–278. doi: 10.5344/ajev.2015.15006

Czemmel, S., Stracke, R., Weisshaar, B., Cordon, N., Harris, N. N., Walker, A. R., et al. (2009). The Grapevine R2R3-MYB Transcription Factor VvMYBF1 Regulates Flavonol Synthesis in Developing Grape Berries. *Plant Physiol.* 151, 1513–1530. doi: 10.1007/s00425-007-0598-8

De Bei, R., Fuentes, S., Gilliham, M., Tyerman, S., Edwards, E., Bianchini, N., et al. (2016). Viticanopy: A Free Computer App to Estimate Canopy Vigor and Porosity for Grapevine. *Sensors* 16, 585. doi: 10.3390/s16040585

de Mendiburu, M. (2016). "Package 'Agricolae.'," in *Statistical Procedures for Agricultural Research. Version 1*.

Gollop, R., Even, S., Colova-Tsolova, V., and Perl, A. (2002). Expression of the Grape Dihydroflavonol Reductase Gene and Analysis of its Promoter Region. *J. Exp. Bot.* 53, 1397–1409. doi: 10.1093/jxb/53.373.1397

Gollop, R., Farhi, S., and Perl, A. (2001). Regulation of the Leucoanthocyanidin Dioxygenase Gene Expression in Vitis Vinifera. *Plant Sci.* 161, 579–588. doi: 10.1016/S0168-9452(01)00445-9

Gómez-Plaza, E., Gil-Muñoz, R., Hernández-Jiménez, A., López-Roca, J. M., Ortega-Regules, A., and Martínez-Cutillas, A. (2008). Studies on the Anthocyanin Profile of Vitis Vinifera Intraspecific Hybrids (Monastrell × Cabernet Sauvignon). *Eur. Food Res. Technol.* 227, 479–484. doi: 10.1007/s00217-007-0744-3

González, C. V., Fanzone, M. L., Cortés, L. E., Bottini, R., Lijavetzky, D. C., Ballaré, C. L., et al. (2015). Fruit-Localized Photoreceptors Increase Phenolic Compounds in Berry Skins of Field-Grown Vitis Vinifera L. Cv. Malbec. *Phytochemistry* 110, 46–57. doi: 10.1016/j.phytochem.2014.11.018

He, F., Mu, L., Yan, G. L., Liang, N. N., Pan, Q. H., Wang, J., et al. (2010). Biosynthesis of Anthocyanins and Their Regulation in Colored Grapes. *Molecules* 15, 9057–9091. doi: 10.3390/molecules15129057

Keller, M. (2020). Developmental Physiology. *The Science of Grapevines Chapter 6: Developmental Physiology. 3rd Edition*, 199–277. San Diego CA, USA, Elsevier Inc. doi: 10.1016/b978-0-12-816365-8.00006-3

Keller, M., Romero, P., Gohil, H., Smithyman, R. P., Riley, W. R., Casassa, L. F., et al. (2016). Deficit Irrigation Alters Grapevine Growth, Physiology, and Fruit Microclimate. *Am. J. Enol. Vitic.* 67, 426–435. doi: 10.5344/ajev.2016.16032

Kobayashi, S., Goto-Yamamoto, N., and Hirochika, H. (2004). Retrotransposon-Induced Mutations in Grape Skin Color. *Science* 304, 982. doi: 10.1126/science.1095011

Kobayashi, S., Ishimaru, M., Hiraoka, K., and Honda, C. (2002). Myb-Related Genes of the Kyoho Grape (Vitis Labruscana) Regulate Anthocyanin Biosynthesis. *Planta* 215, 924–933. doi: 10.1007/s00425-002-0830-5

Kurtural, S. K., and Gambetta, G. A. (2021). Global Warming and Wine Quality: Are We Close to the Tipping Point? *Oeno One* 55, 353–361. doi: 10.20870/oeno-one.2021.55.3.4774

Martínez-Lüscher, J., Brillante, L., and Kurtural, S. K. (2019). Flavonol Profile is a Reliable Indicator to Assess Canopy Architecture and the Exposure of Red Wine Grapes to Solar Radiation. *Front. Plant Sci.* 10. doi: 10.3389/fpls.2019.00010

Martínez-Lüscher, J., Chen, C. C. L., Brillante, L., and Kurtural, S. K. (2017). Partial Solar Radiation Exclusion With Color Shade Nets Reduces the Degradation of Organic Acids and Flavonoids of Grape Berry (Vitis vinifera L.). *J. Agric. Food Chem.* 65, 10693-10702. doi: 10.1021/acs.jafc.7b04163

Martínez-Lüscher, J., Sánchez-Díaz, M., Delrot, S., Aguirreolea, J., Pascual, I., and Gomès, E. (2014a). Ultraviolet-B Radiation and Water Deficit Interact to Alter Flavonol and Anthocyanin Profile in Grapevine Berries Through Transcriptomic Regulation. *Plant Cell Physiol.* 55, 1925–1936. doi: 10.1093/pcp/pcu121

Martínez-Lüscher, J., Torres, N., Hilbert, G., Richard, T., Sánchez-Díaz, M., Delrot, S., et al. (2014b). Ultraviolet-B Radiation Modifies the Quantitative and Qualitative Profile of Flavonoids and Amino Acids in Grape Berries. *Phytochemistry* 102, 106–114. doi: 10.1016/j.phytochem.2014.03.014

Matus, J. T. (2016). Transcriptomic and Metabolomic Networks in the Grape Berry Illustrate That it Takes More Than Flavonoids to Fight Against Ultraviolet Radiation. *Front. Plant Sci.* 7. doi: 10.3389/fpls.2016.01337

Mori, K., Goto-Yamamoto, N., Kitayama, M., and Hashizume, K. (2007). Loss of Anthocyanins in Red-Wine Grape Under High Temperature. *J. Exp. Bot.* 58, 1935–1945. doi: 10.1093/jxb/erm055

Movahed, N., Pastore, C., Cellini, A., Allegro, G., Valentini, G., Zenoni, S., et al. (2016). The Grapevine VviPrx31 Peroxidase as a Candidate Gene Involved in Anthocyanin Degradation in Ripening Berries Under High Temperature. *J. Plant Res.* 129, 513–526. doi: 10.1007/s10265-016-0786-3

Ponce de León, M. A., and Bailey, B. N. (2021). A 3D Model for Simulating Spatial and Temporal Fluctuations in Grape Berry Temperature. *Agric. For. Meteorol.* 306, 1–11. doi: 10.1016/j.agrformet.2021.108431

Rana, G., Katerji, N., Introna, M., and Hammami, A. (2004). Microclimate and Plant Water Relationship of the "Overhead" Table Grape Vineyard Managed With Three Different Covering Techniques. *Sci. Hortic.* 102, 105–120. doi: 10.1016/j.scienta.2003.12.008

Reshef, N., Walbaum, N., Agam, N., and Fait, A. (2017). Sunlight Modulates Fruit Metabolic Profile and Shapes the Spatial Pattern of Compound Accumulation Within the Grape Cluster. *Front. Plant Sci.* 8. doi: 10.3389/fpls.2017.00070

Robson, T. M., Klem, K., Urban, O., and Jansen, M. A. K. (2015). Re-Interpreting Plant Morphological Responses to UV-B Radiation. *Plant Cell Environ.* 38, 856–866. doi: 10.1111/pce.12374

Savoi, S., Wong, D. C. J., Degu, A., Herrera, J. C., Bucchetti, B., Peterlunger, E., et al. (2017). Multi-Omics and Integrated Network Analyses Reveal New Insights Into the Systems Relationships Between Metabolites, Structural Genes, and Transcriptional Regulators in Developing Grape Berries (Vitis Vinifera L.) Exposed to Water Deficit. *Front. Plant Sci.* 8. doi: 10.3389/fpls.2017.01124

Spayd, S. E., Tarara, J. M., Mee, D. L., and Ferguson, J. C. (2002). Separation of Sunlight and Temperature Effects on the Composition of Vitis Vinifera Cv. Merlot Berries. *Am. J. Enol. Vitic* 53:171–82. doi: 10.1021/jf970988p

Sweetman, C., Sadras, V. O., Hancock, R. D., Soole, K. L., and Ford, C. M. (2014). Metabolic Effects of Elevated Temperature on Organic Acid Degradation in Ripening Vitis Vinifera Fruit. *J. Exp. Bot.* 65, 5975–5988. doi: 10.1093/jxb/eru343

Torres, N., Martínez-Lüscher, J., Porte, E., and Kurtural, S. K. (2020). Optimal Ranges and Thresholds of Grape Berry Solar Radiation for Flavonoid Biosynthesis in Warm Climates. *Front. Plant Sci.* 11. doi: 10.3389/fpls.2020.00931

Torres, N., Martínez-Lüscher, J., Porte, E., Yu, R., and Kaan Kurtural, S. (2021). Impacts of Leaf Removal and Shoot Thinning on Cumulative Daily Light Intensity and Thermal Time and Their Cascading Effects of Grapevine (Vitis

vinifera L.) Berry and Wine Chemistry in Warm Climates. *Food Chem.* 343, 128447. doi: 10.1016/j.foodchem.2020.128447

Torres, N., Yu, R., Martinez-Luscher, J., Girardello, R. C., Kostaki, E., Oberholster, A., et al. (2022). Shifts in the Phenolic Composition and Aromatic Profiles of Cabernet Sauvignon (Vitis vinifera L.) Wines are Driven by Different Irrigation Amounts in a Hot Climate. *Food Chem.* 371, 10693–702. doi: 10.1016/j.foodchem.2021.131163

Vitrac, X., Larronde, F., Krisa, S., Decendit, A., Deffieux, G., and Mérillon, J. M. (2000). Sugar Sensing and Ca2+-Calmodulin Requirement in Vitis vinifera Cells Producing Anthocyanins. *Phytochemistry* 53, 659–665. doi: 10.1016/S0031-9422(99)00620-2

Walker, A. R., Lee, E., Bogs, J., McDavid, D. A. J., Thomas, M. R., and Robinson, S. P. (2007). White Grapes Arose Through the Mutation of Two Similar and Adjacent Regulatory Genes. *Plant J.* 49, 772–785. doi: 10.1111/j.1365-313X.2006.02997.x

Waterhouse, A. L., Sacks, G. L., and Jeffery, D. W. (2016). *Understanding Wine Chemistry* The Atrium, Southern Gate, Chichester, West Sussex United Kingdom: John Wiley & Sons, Ltd. doi: 10.1002/9781118730720

Wu Dai, Z., Meddar, M., Renaud, C., Merlin, I., Hilbert, G., Delro, S., et al. (2014). Long-Term *In Vitro* Culture of Grape Berries and Its Application to Assess the Effects of Sugar Supply on Anthocyanin Accumulation. *J. Exp. Bot.* 65, 4665–4677. doi: 10.1093/jxb/ert489

Conflict of Interest: The authors declare that the research was conducted in the absence of any commercial or financial relationships that could be construed as a potential conflict of interest.

Publisher's Note: All claims expressed in this article are solely those of the authors and do not necessarily represent those of their affiliated organizations, or those of the publisher, the editors and the reviewers. Any product that may be evaluated in this article, or claim that may be made by its manufacturer, is not guaranteed or endorsed by the publisher.